Frequenz, Vol. **65** (2011), pp. 201–207 DOI 10.1515/FREQ.2011.028

A 77 GHz Near-Field Probe with Integrated Illuminating Waveguide used for Reflectarray Characterization

Sabine Dieter,[1,*] **Simone Montori,**[2] **Zimeng Yang,**[1] **Roberto Sorrentino**[2] **and Wolfgang Menzel**[1]

[1] Institute of Microwave Techniques, University of Ulm, 89081 Ulm, Germany

[2] Department Electronic and Information Engineering, University of Perugia, Perugia Italy

Abstract. In this paper, a near-field probe with integrated illuminating waveguide for frequencies around 77 GHz is introduced. For such high frequencies, alignment of transmitter and receiver probes in the near-field measurement setup are difficult. So the purpose of this work is to integrate both devices into one setup for an easy and reproducible measurement procedure. The measurement probe is used to characterize individual patches on the surface of reflectarray antennas, placing the device a few millimeters above the antenna surface. This requires a high spatial resolution and a insignificant influence of the probe on the examined structure. The ability of the developed probe has been investigated in simulations and verified in near-field measurements at reflectarray structures for 77 GHz. In this extended paper version, the setup is used to investigate a test-array with polarization twisting elementary cells and the lower reflector of a folded antenna, whose characteristics are based on a bifocal design process.

Keywords. Near-field characterization, high resolution probe, reflectarray antenna.

PACS®(2010). 84.40.-x, 07.57.-c, 84.40.Ba.

1 Introduction

Reflectarray antennas [1–3] have the advantages of easy, low-cost fabrication and high gain. Simulation tools for these antennas are usually based on Frequency Selective Surface Simulations (FSS), which assume infinite periodic structures.

In order to examine the realistic behavior of such antennas, including the necessary geometrical variations, finite dimensions, edge effects, and errors due to fabrication tolerances as well, different characterization methods [4] have been developed in recent time. These methods may also be applied within other measurement applications, e.g. for the characterization of reconfigurable antenna concepts [4] or for other setups in the microwave frequency range.

The problem with rising frequency, however, is the decreasing size of both the examined structure and the measurement devices. Near-field measurement concepts introduced for frequencies around 35 GHz [5] are not easily applicable for higher frequencies, where the designer has to deal with problems of increased errors due to fabrication tolerances within the probe design. Another challenge in higher frequency regions is the alignment of the measurement devices in the near-field setup, leading to shadowing effects and multiple reflections.

In order to overcome these problems, a novel high-resolution near-field probe is introduced in this paper. This device combines both illuminating waveguide and detecting probe for 77 GHz, reduces the alignment problem, and offers reproducible measurement results.

2 Principle of the Probe

The probe design is based on a substrate integrated waveguide (SIW) [6]. This consists of a dielectric material metalized on top and bottom. Two rows of metalized via holes are used as waveguide boundaries. An enlarged photograph of a SIW for 77 GHz is shown in Figure 1.

The used substrate (Rogers RT Duroid 6010) has a high permittivity of $\varepsilon_r = 10.8$, the substrate thickness is $h = 0.64$ mm. This allows small waveguide dimensions and therefore leads to the desired high spatial resolution of the probe.

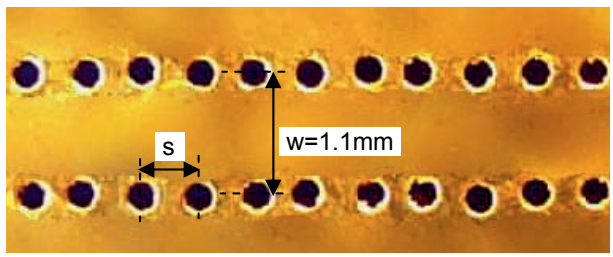

Figure 1. Top view of a fabricated substrate-integrated waveguide (SIW).

Corresponding author: Sabine Dieter, Institute of Microwave Techniques, University of Ulm, 89081 Ulm, Germany;
E-mail: sabine.dieter@uni-ulm.de.

Received: June 19, 2011.

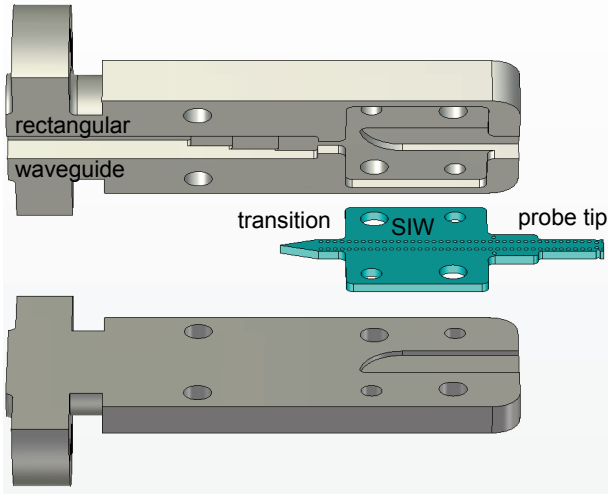

Figure 2. Open simulation model of a near-field probe.

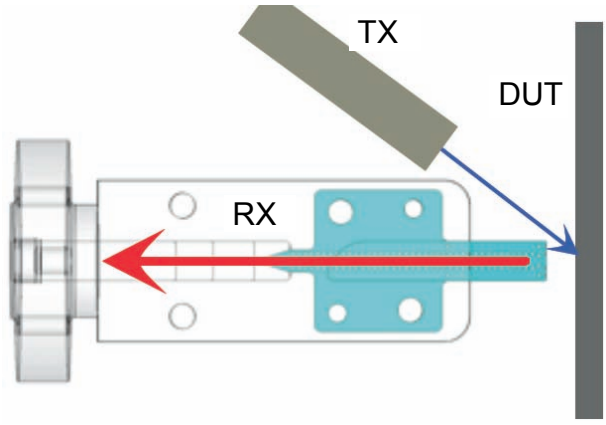

Figure 3. Near-field measurement principle with separated waveguide for illumination (TX) and detecting probe (RX).

The geometrical parameters of the SIW also depend on the fabrication tolerances, such as increased deviations for the placement of the drill holes with smaller repetition distances s.

Here, the via hole diameter is chosen to $d = 0.3$ mm, the via distance (SIW width) is $w = 1.1$ mm, and the via repetition distance is $s = 0.5$ mm.

The effective width w_{eff} of the waveguide was determined by simulations of a SIW with the parameters mentioned above, and compared to an equivalent waveguide model with electric walls as waveguide boundaries [7]. The result for the effective width obtained with this model was $w_{\text{eff}} = 0.914$ mm. This result is consistent with the estimation from [8] for the SIW parameters from above, which leads to $w_{\text{eff}} = 0.9$ mm.

The principle of a SIW probe design without integrated illumination is shown in Figure 2. The probe consists of a rectangular waveguide with a transition to SIW. This reduces stepwise the height of the rectangular waveguide down to the substrate thickness $h = 0.64$ mm. The substrate at the transition itself has the shape of an arrow, which leads to a slower change of the effective permittivity at the transition.

As mentioned above, the high permittivity of the substrate allows small effective waveguide dimensions and good spatial resolution of the probe. As a drawback of this high permittivity, one should mention the increased substrate losses and the high permittivity steps to air which lead to strong reflections.

3 Measurement Setup and Integration of the Transmitting Waveguide

The measurement setup with a probe as described above is shown in Figure 3. An open waveguide (TX) is illuminating the device under test (DUT), which here is a reflectarray surface. The reflected field component is detected by the probe (RX), a few millimeters above the DUT's surface.

Although Figure 3. only shows the measurement principle, it is easy to imagine the problems of alignment of the devices in the near-field measurement setup, possibly leading to shadowing effects, multiple reflections, and a slant angle of incidence.

The alternative probe design proposed in this paper is shown in Figure 4. It combines both illuminating waveguide (TX) and detecting probe (RX). To this end, a dielectric substrate with the probe is suspended centrally in the H-plane of the illuminating waveguide. The probe itself protrudes out of the waveguide; within the waveguide arrangement, a transition to standard waveguide is integrated. The transmit signal is fed into the structure via waveguide bend and radiates from the open space above and below the probe substrate.

The integration of the probe reduces the alignment problem and allows reproducible measurement results.

4 Simulation and Fabrication of the Probe

In order to obtain the overall model of the probe, simulation models of the single parts have been built, and their parameters have been optimized separately according to [7]. All sub-models have been combined to the final probe version, as it can be seen in Figure 4. This includes a model for the SIW, one model for the RX-transition between waveguide and air, and for the behavior of the probe tip in front of an electric wall. With respect to the transmitting waveguide (TX), the purpose is to both illuminate the DUT from above and below the probe, but in a bigger distance than the probe tip. So the height of the transmitter waveguide is increased stepwise, and finally, the waveguide is separated into two

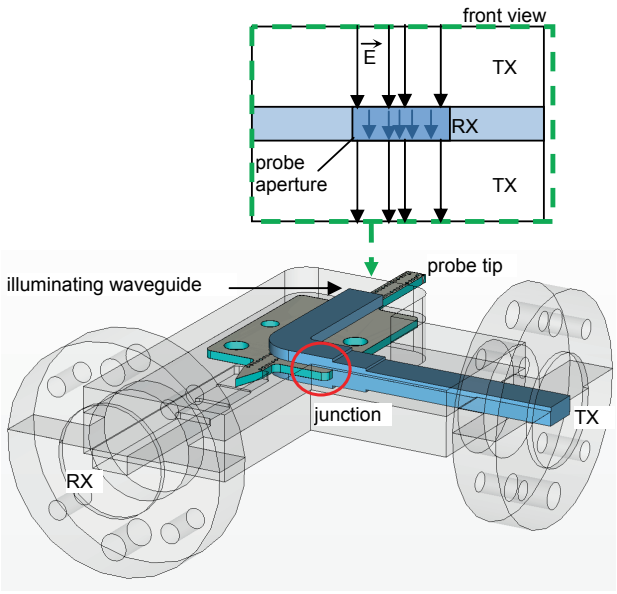

Figure 4. Simulation model of detecting probe with integrated illuminating waveguide for 77 GHz.

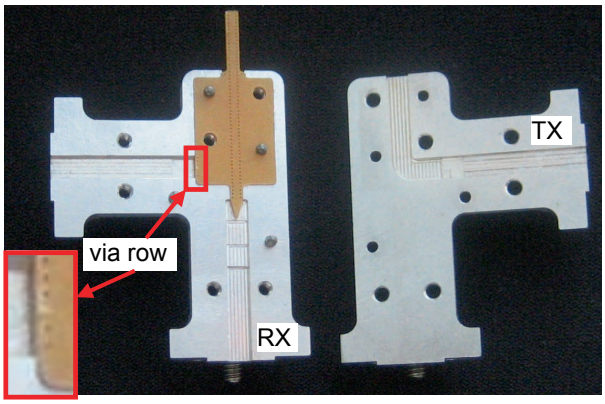

Figure 5. Opened integrated probe for 77 GHz.

parts at the junction. To prevent the transmitted wave from leaking into the side wings of the SIW substrate, an additional via row was added in the substrate at the junction point, see Figure 5, showing the opened fabricated arrangement.

The simulated and measured return loss of the critical RX-path is shown in Figure 6. Obviously the SIW structure suffers from high losses due to an increased electrical length of the high-permittivity substrate, especially for the integrated probe, which has increased dimensions compared to the detect-only probe, see Figure 7 (A). Due to the high computational effort for the simulation of the whole model, the substrate losses were neglected in the simulation. Another drawback of the probe is the resonant length leading to standing waves, due to high permittivity steps at the interfaces to air.

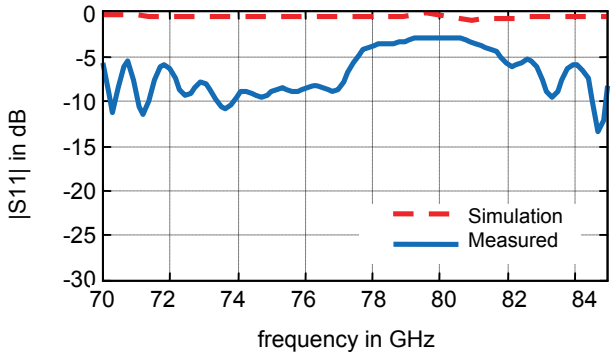

Figure 6. Simulated and measured return loss of the fabricated probe.

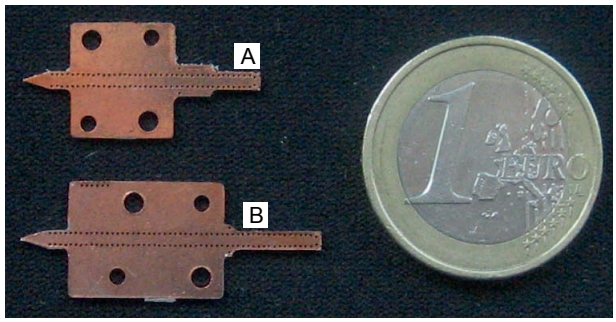

Figure 7. Fabricated substrate-integrated waveguides for the detect-only probe (A) and for the integrated probe (B).

However, the probe is still able to detect signals in the near-field. So the advantages of small waveguide dimensions are settling the choice of the substrate type.

5 Near-Field Measurement Results

For the verification of the probe, a test reflectarray has been fabricated as a DUT and examined in the near-field setup. The test structure includes four sub-regions, all consist of patch arrays with the same dimensions, but rotated by 90° respectively (see Figure 8). The dimensions of the patches are chosen in such a way that there is a phase angle difference of 180° between both orientations.

The patch positions and the phase angle differences should be verified in the measurement setup, which can be seen in Figure 9. The illumination of the DUT occurs in the far-field, from above and below the probe. The probe tip itself is situated in the near-field of the array, detecting the reflected signal components from the test array. During the measurement, the location of the array is controlled automatically via an x-y-table.

The respective measurement results in amplitude and phase of the near-field of the scanned array are shown in Figure 10 and Figure 11. In the amplitude scan (Figure 10),

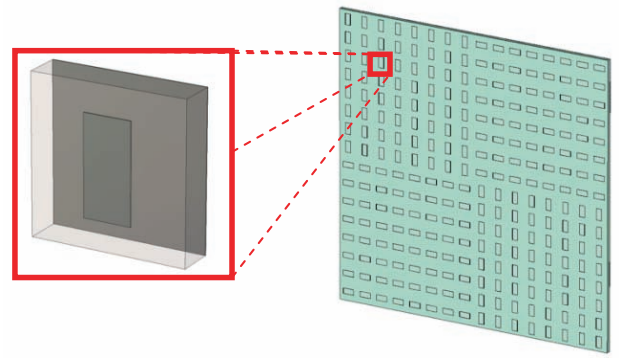

Figure 8. Model of the test reflectarray for verification of the probe.

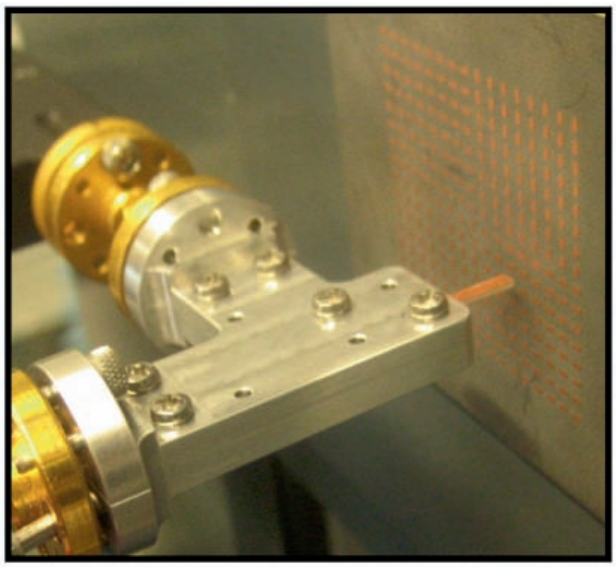

Figure 9. Measurement setup with integrated probe and test reflectarray.

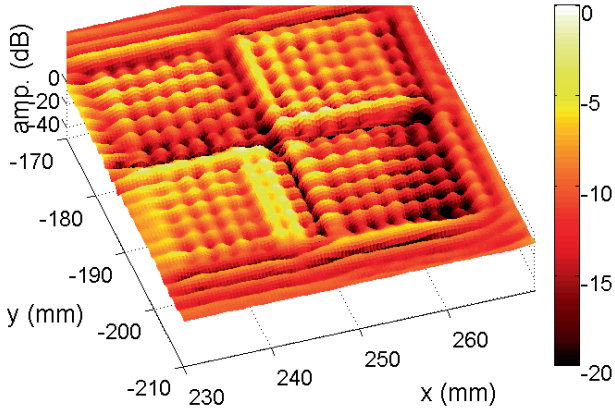

Figure 10. Measured amplitude result of the test structure.

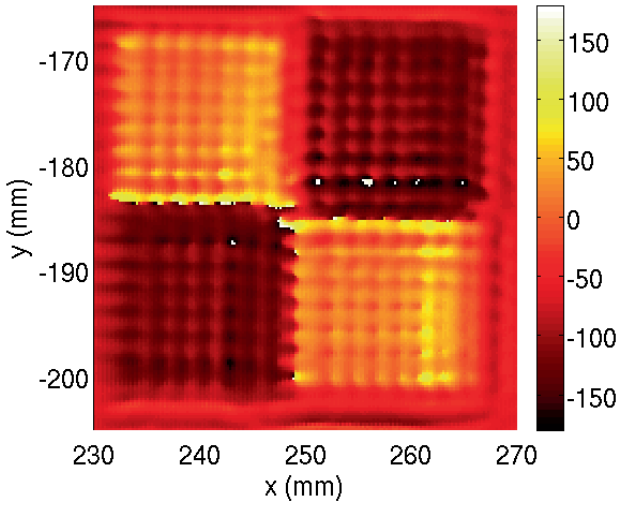

Figure 11. Measured phase angle result of the test structure.

one can see that the resolution of the probe is high enough to separate each single patch on the reflector. The correspondent phase angle result obtains the expected phase angle difference of 180° between the patch regions.

6 Polarization Turning Elementary Cell Measurement Results

A further verification of the high resolution near-field probe proposed in this work has been performed testing the 1-bit reconfigurable elementary cell developed in the frame of the ARASCOM project ("MEMS & Liquid Crystal based Agile Reflectarray Antennas for Security & COMmunication") [9]. One of the aims of the project is the development of a 76.5 GHz imaging system for security applications based on a large reconfigurable reflectarray. The principle of operation of elementary cell (Figure 13) is based on the polarization twisting concept: the MEMS-controlled phase shifting layer provides a $\pm 90°$ geometrical rotation of the incident field, in this way is possible to obtain a relative phase difference of 0°/180° for a theoretically unlimited bandwidth [10].

A 16×16 test reflectarray has been manufactured as a DUT and examined in the near-field setup. All the cells included in the reflectarray are in the same configuration and the MEMS have been replaced by short/open connections. Also in this case the patch positions and the phase angle differences should be verified.

Since ARASCOM elementary cell reflect a polarization orthogonal respect to the received one, the measurement setup with separated waveguides as shown in Figure 3 has been used, but in this case, the far-field illumination of the DUT (TX) is performed using a 90° twisted waveguide, see Figure 14.

The amplitude measurement results of the scanned array (Figure 15) show that is possible to precisely distinguish

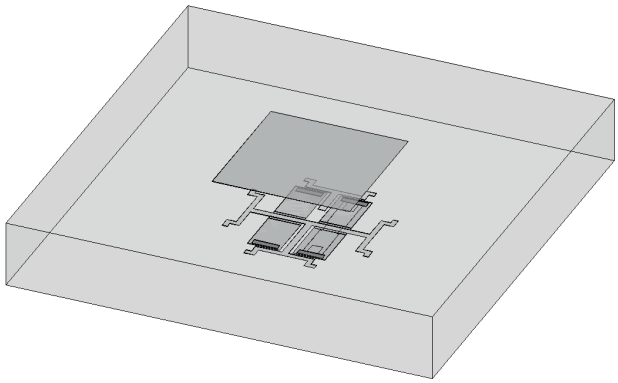

Figure 12. Perspective view of ARASCOM elementary cell.

Figure 14. Picture of measurement setup for the ARASCOM cell.

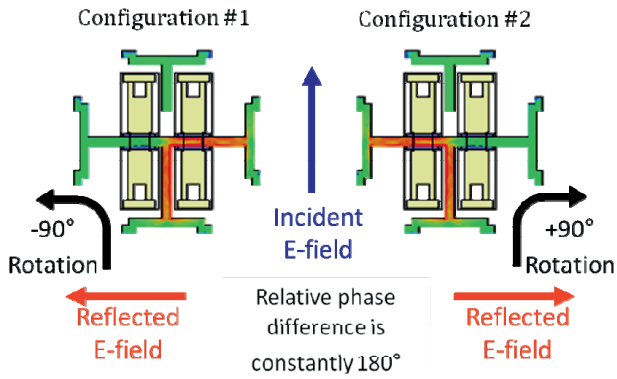

Figure 13. Principle of operation of elementary cell.

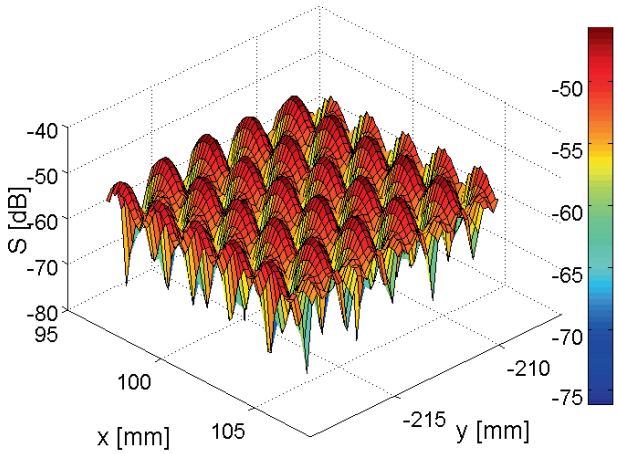

Figure 15. Amplitude of the detected signal.

the position of each patch on the array confirming the high resolution of the near-field probe.

Exploiting the symmetry of the elementary cell, the two possible configurations are obtained by rotating the DUT by 90°between two measurements. Some phase angle results for both configurations are shown in Table I. The phase angle difference between the two possible configurations has been evaluated at the patch locations and shows an average value of 178°. The obtained value of relative phase difference is only 2° away from the optimal value of 180° and is almost the same value obtained in the free space measurement setup described in [10].

7 Phase Angle Measurement Results of a Reflectarray Antenna

The integrated probe setup, as shown in Figure 9, has been used to characterize a folded reflectarray antenna [2]. Figure 16 shows the cross section and rays of a modified folded reflectarray antenna. The radiation from the feed is incident on a planar structure on top which, in the modified version, includes a grid on the outer side and narrow dipoles paral-

	Patch #1	Patch #2	Patch #3	Patch #4	Patch #5	Patch #6	Patch #7	Patch #8	Mean value:
Conf. #1	127.7°	127.9°	130.1°	131.8°	134°	139.7°	130.5°	132.4°	131.1°
Conf. #2	−46.5°	−44.7°	−49.8°	−51.3°	−42.5°	−53.6°	−44.4°	−46.9°	−47.3°
Average Relative phase difference:									178.4°

Table 1. Reflected phase evaluated in correspondence of 8 randomly selected patch locations.

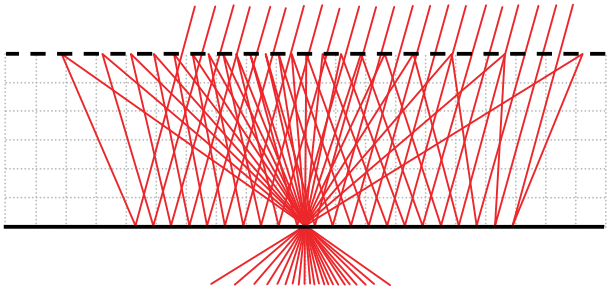

Figure 16. Raytracing for the investigated folded reflectarray antenna.

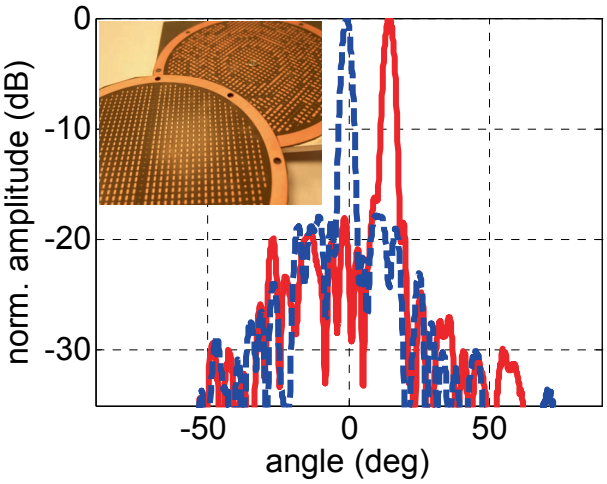

Figure 17. Measured far-field diagram in the E-plane of the antenna at 77 GHz with grid design for main beam directions 0° and 14°.

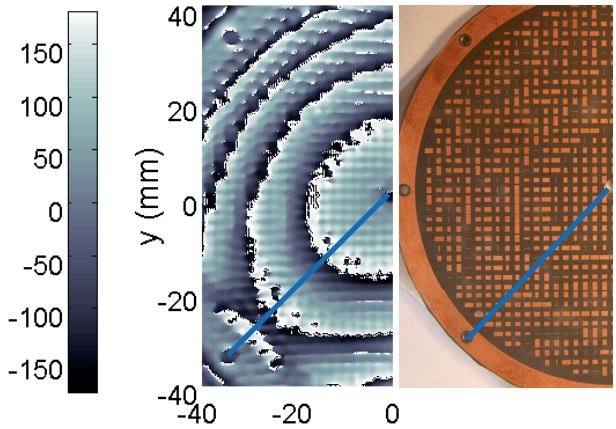

Figure 18. Measured phase angle result of a near-field scan with the integrated probe of the lower reflector at 77 GHz and photo of the lower reflector.

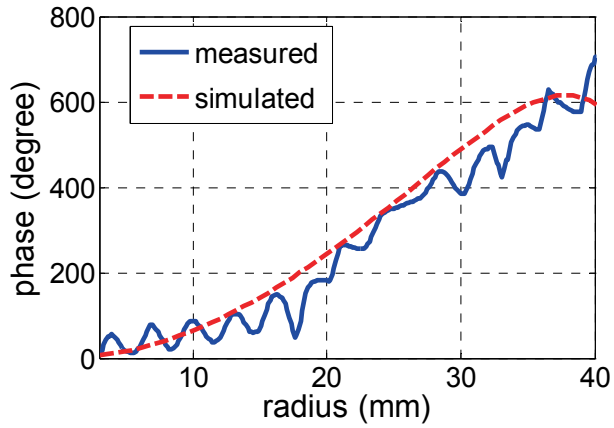

Figure 19. Measured and simulated phase angle for a radial cut of the antenna reflector in the bifocal axis at 77 GHz.

lel to the grid on the inner side [11]. Thus, this configuration acts both as a polarizing filter and a reflectarray for the polarization parallel to grid and dipoles, reflecting the feed radiation with a controlled phase angle adjustment. At the reflectarray on the lower side, phase angle can be adjusted again, and polarization is twisted by 90°. Based on the principle of bifocal antennas, this configuration can be designed as multibeam antenna [11] or, with variable phase adjustment at the upper reflector, as scanning antenna [12]. Phase variation on the upper reflector can, for example, be achieved on the basis of liquid crystal material [4].

The performance of the later concept has been tested with two upper substrates in a "frozen" state for beam-steering directions 0° and 14° based on standard Rogers RT5880 substrates with half a millimeter thickness [12]. The measured far-field diagrams in the E-plane for the two designs are shown in Figure 17. The respective antenna gains are 31.8 dBi and 30 dBi.

In this work, the lower phase angle distribution is investigated in the above mentioned near-field measurement setup with the integrated probe at 77 GHz. In Figure 18, the phase angle result of a measured near-field scan above the lower reflector is shown. The phase angle results show reasonable results and even the drill holes can be detected easily with the given setup. A radial cut is marked in Figure 18, both in the measured phase angle plot and the photo of the reflector.

The measured phase angle results in this radial scan are compared with the theoretical phase angles from the design process and are shown in Figure 19. It can be seen, that the theoretically required reflection phase angles are verified by the measurement results achieved with the proposed near-field measurement setup.

8 Conclusion

In this paper, a high resolution near-field probe with integrated illuminating waveguide is proposed. The probe design and near-field measurement setup for 77 GHz have been shown and verified for a test array at this frequency.

The measurement setup using this probe reduces the alignment problem and allows reproducible measurement results. Due to the high resolution and the small influence of the probe, the patches could be detected individually, and the designed phase angle differences between the patch regions could be verified.

Furthermore, the setup has been used to investigate a test-array with polarization twisting elementary cells and the lower reflector of a folded reflectarray antenna, whose characteristics is based on a bifocal design process.

Acknowledgments

This work has been funded by the German Research Association DFG under the contract ME 1016/14-2 The development of elementary cell in paragraph VI has been performed in the frame of the ARASCOM project supported by the 7th European framework program, contract no. 222620.

References

[1] D. M. Pozar, S. D. Targonski, H. D. Syrigos, "Design of millimeter wave microstrip reflectarrays", *IEEE Trans. on Antennas and Propagation*, vol. AP-45 (1997), pp. 287–296.

[2] W. Menzel, D. Pilz, M. Al-Tikriti, "MM-Wave Folded Reflector Antennas with High Gain, Low Loss, and Low Profile", *IEEE AP Magazine, June 2002*, pp. 24–29.

[3] J. A. Zornoza, R. Leberer, M. Moraga, J. A. Encinar, W. Menzel, "A folded 3-layer printed reflectarray with shaped pattern for LMDs central station sectored antenna", *IEEE Int.Symposium on Antennas and Propagation*, Monterey, USA, July 2004, Vol. 1, pp. 5–8.

[4] S. Dieter, A. Moessinger, S. Mueller, W. Menzel, R. Jakoby, "Characterization of Reconfigurable LC Reflectarrays Using Near-Field Measurements", *in Proc. Of 4th German Microwave Conference (GeMiC)*, 2009, Mar. 16–18, pp. 1–4.

[5] S. Dieter, W. Menzel, "High Resolution Probes for Near-Field Measurements of Reflectarray Antennas", *in IEEE Antennas and Wireless Propagation Letters*, Vol. 8 (2009), pp. 157–160.

[6] D. Deslandes, K. Wu, "Integrated microstrip and rectangular waveguide in planar form," *IEEE Microwave Wireless Component Letters*, vol. 11 (2001), no. 2, pp. 68–70.

[7] CST AG: CST Microwave Studio 2009, Darmstadt Germany, Jan 2009.

[8] F. Xu, K. Wu, "Guided-Wave and Leakage Characteristics," *IEEE Trans. on Microwave Theory and Techniques*, Vol. 53, No.1 (2005), pp. 66–73.

[9] `www.arascom.eu`

[10] S. Montori, C. Fritzsch, L. Marcaccioli, R. V. Gatti, R. Jakoby, R. Sorrentino, "Design and measurements of a 1-bit reconfigurable elementary cell for large electronic steerable reflectarrays", European Microwave Conference (EuMC), 2010, pp. 918–921.

[11] W. Menzel, M. Al-Tikriti, R. Leberer, *"A 76 GHz multiple-beam planar reflector antenna"*, European Microw. Conf., Milano, Italy, Sept. 2002, pp. 977–980 (Vol. III).

[12] S. Dieter, P. Feil, and W. Menzel, "Folded Reflectarray Antenna Using A Modified Polarization Grid for Beam-Steering," *Proc. of 5th European Conference on Antennas and Propagation (EuCAP)*, 2011, Apr. 2011, pp. 1486–1489.